PAPER

Check for updates

Hydrophobic nanofibers: a peptide-based functional anti-fouling material†

Kshitish Chandra Hati,‡[a] Santosh Kumar,‡[a] Sahabaj Mondal,[a] Surajit Singh,[a] Ananda Shit,[a] Sujay Kumar Nandi[a] and Debasish Haldar [ID] *[ab]

Functional bioinspired materials have been developed by molecular self-assembly of a hydrophobic peptide. Two analogue peptides containing hydrophobic L-alanine, α-aminoisobutyric acid (Aib), L-phenylalanine and L-tyrosine deliver different supramolecular structures and functions. Peptide **1** containing L-phenylalanine adopts a β-turn conformation and self-assembles through intermolecular hydrogen bonds to form a supramolecular hydrophobic sheet-like structure. But peptide **2** with L-tyrosine adopts kink-like conformations and self-assembles to form a supramolecular hydrogen bonded helix-like architecture. Irrespective of the presence of the same peptide backbone conformation, only the side chain hydroxyl functional group has introduced a huge change in self-assembly pattern and function. The hydrophobic peptide **1** further self-assembled to form slippery nanofibers. The resulting surfaces show anti-sticking effects against water and exhibit anti-fouling properties, like inhibiting the growth of *Escherichia coli*.

Introduction

In nature, plenty of plants, insects and animals have slippery self-cleaning surfaces which are able to repel water and exhibit anti-fouling properties. There are many species that exhibit surface properties such as secretion of wax, gum, oil, toxins or mucus for sustainability.[1] Even invertebrates like mollusca and cnidaria exhibit surface properties and clean their bodies from soil, dust and debris by perpetually discharging mucus.[2] The lotus leaves exhibit excellent water repellence by making the surface super hydrophobic using wax.[3] The fouling of surfaces has wide effects. Various approaches have been developed to design anti-fouling surfaces. The fabrication of novel anti-fouling materials inspired by natural systems, using the self-assembly of synthetic organic moieties is highly interesting due to their potential application in bioorganic chemistry, medicine and material sciences.[4,5] Recently Lynn's group have developed an anti-fouling coating that can host and sustain the release of water-soluble agents.[6] Hozumi and coworkers have developed

self-lubricating organogels with exceptional anti-sticking properties against viscous emulsions.[7] The self-assembly process requires a combination of several noncovalent interactions[8] such as hydrogen bonding, π–π stacking, and van der Waals interactions between the building blocks and can be tuned by different external stimuli like pH, concentration, heat, light radiation, addition of salts and solvent polarity.[9–16]

Different building blocks such as urea, amides, peptides, nucleobases and carbohydrates have shown spectacular abilities to form supramolecular gels. The gels have wide applications such as removal of toxic dyes, oils and metal ions from water;[17–24] as catalysts,[25,26] dye sensitized solar cells,[27] and matrices for nanoparticle synthesis;[28–32] and in drug delivery systems.[33–35] In this context, a small peptide scaffold that can serve as a hydrogen bond donor or acceptor is highly interesting.[36] In particular, we are interested in tripeptide-based scaffolds due to their structural versatility, biocompatibility, robustness, and accessibility by standard analytical methods.[37]

Herein, we explore the use of tripeptides as building blocks for the formation of functional bioinspired materials. X-ray crystallography sheds some light on the conformations and self-assembly propensities of the tripeptides. Peptide **1** containing L-Phe forms a ten-member intramolecular hydrogen-bonded β-turn conformation and self-assembles through intermolecular hydrogen bonds to form supramolecular sheet-like structures. Whereas the tyrosine analogue adopts a kink-like conformation and self-assembles to form a supramolecular helical architecture. Moreover, the hydrophobic

[a] *Department of Chemical Sciences, Indian Institute of Science Education and Research Kolkata, Mohanpur-741246, West Bengal, India.*
E-mail: deba_h76@yahoo.com, deba_h76@iiserkol.ac.in

[b] *Centre for Advanced Functional Materials (CAFM), Indian Institute of Science Education and Research, Kolkata, Mohanpur-741246, West Bengal, India*

† Electronic supplementary information (ESI) available: Fig. S1–S9, Table S1–S6, Synthesis, and characterizations (Fig. S10–S16). CCDC 2106154 and 2106153. For ESI and crystallographic data in CIF or other electronic format see DOI: https://doi.org/10.1039/d2ma00084a
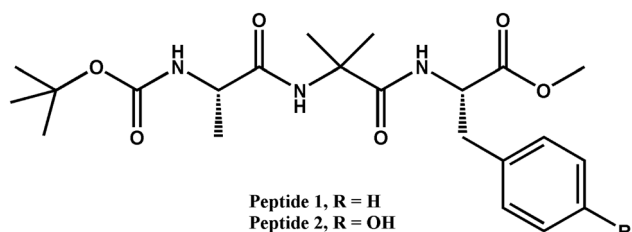
‡ Have equal contribution.

peptide **1** further self-assembles to form slippery nanofibers. The resulting surfaces show an anti-sticking effect against water and exhibit anti-fouling properties, like inhibiting the growth of *Escherichia coli*.

Results and discussion

We have designed and synthesized two tripeptides. The peptides contain L-Ala at the N-terminus, a helicogenic Aib residue at the center and Phe/Tyr at the C-terminus (Scheme 1).[38] The central helicogenic Aib residue may help to form a turn-like structure. The strong intermolecular hydrogen bonding and π–π stacking interactions between the side chains may dictate the assembly pattern. Target tripeptides **1** and **2** were synthesized by conventional solution phase reaction using DCC/HOBT as the coupling reagent. The final compounds were purified by column chromatography and characterized by ^{1}H-NMR, ^{13}C-NMR, FT-IR spectroscopy and mass spectrometry.

First, the self-assembly of the tripeptides was examined by solid FT-IR spectroscopy. In FT-IR, the region 3500–3200 cm^{-1} is responsible for the N–H stretching vibrations and 1800–1600 cm^{-1} corresponds to the C=O stretching vibration of the amide and ester groups. The FT-IR spectra (Fig. 1) of the peptides **1** and **2** exhibit N–H stretching frequencies at 3270 and 3356 cm^{-1} respectively, responsible for hydrogen bonded N–H stretching. The band at 3450 cm^{-1} appeared for non hydrogen-bonded N–H. For tripeptide **1**, the ester and amide peaks appeared at 1682 and 1630 cm^{-1}. The tripeptide **2** exhibits peaks at 1690 and 1645 cm^{-1}. We conclude that both tripeptides **1** and **2** have similar hydrogen bonded structures in the solid state.

Furthermore, the structure and self-assembly pattern of the tripeptides **1** and **2** have been studied by single-crystal X-ray diffraction analysis. The colorless monoclinic crystals of tripeptides Boc-Ala-Aib-Phe-OMe (tripeptide **1**) and Boc-Ala-Aib-Tyr-OMe (tripeptide **2**) suitable for crystallography were obtained from methanol-water solution by slow evaporation. The molecular conformations of tripeptide **1** in the crystal state are illustrated in Fig. S1 (ESI†). Most of the backbone dihedral angle ϕ and ψ values (except $\phi1$ and $\psi3$) of the constituent amino acid residues of tripeptide **1** fall within the helical region of the Ramachandran plot. The important backbone dihedral angles of tripeptide **1** are listed in Table S1 (ESI†). The tripeptide **1** forms an intramolecular hydrogen bonded β-turn conformation (N3–H3···O2) (Table S2, ESI†). The ORTEP diagram
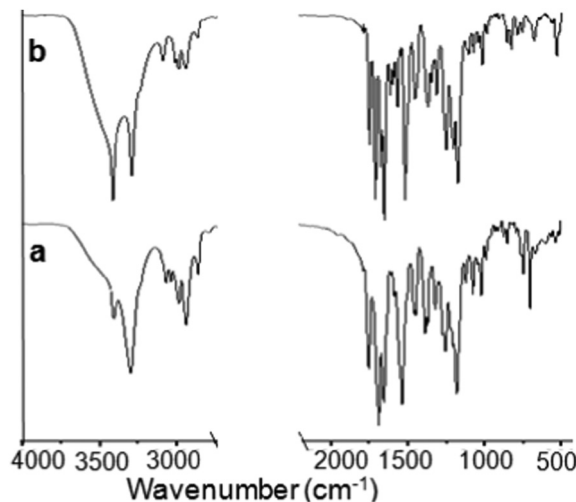

Fig. 1 Solid state FT-IR spectra of peptides (a) **1** and (b) **2**.

of peptide **2** with the atom numbering scheme is presented in Fig. S2 (ESI†). In the crystal, peptide **2** is unable to form any intramolecularly hydrogen bonded β-turn structure though the ϕ and ψ values of the constituent amino acid residues fall within the type II β-turn region of the Ramachandran map. The important backbone dihedral angles of tripeptide **2** are listed in Table S4 (ESI†). We have compared the molecular conformations of peptide **1** and peptide **2** (Fig. 2a). From Fig. 2a, the backbone conformations of peptides **1** and **2** are almost the same. The β-turn conformations of tripeptide **1** further self-assemble through the intermolecular hydrogen

Scheme 1 Schematic presentation of tripeptides **1** and **2**.
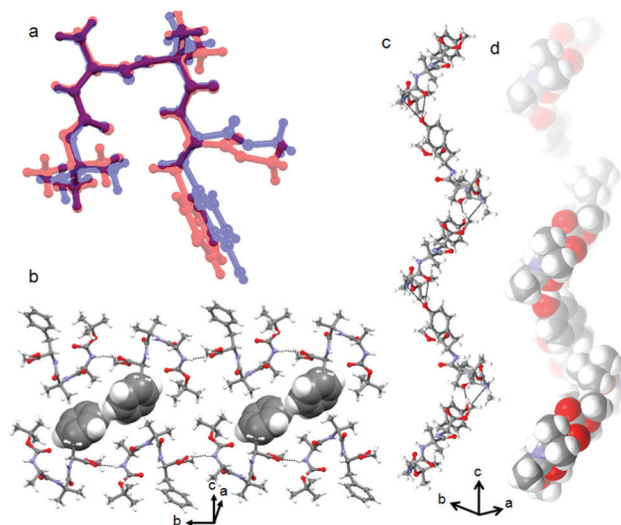
Peptide 1, R = H
Peptide 2, R = OH

Fig. 2 (a) The superposition of the tripeptides **1** (red) and **2** (blue) clearly exhibits the almost same conformations in the solid-state. (b) The supramolecular β-sheet structure of tripeptide **1** along the crystallographic *b* and *c* axis. Hydrogen bonds are shown as black dotted lines. Edge to edge π–π stacking is shown by the space fill model. (c) The supramolecular helical structure of tripeptide **2** along the crystallographic *c* axis in a ball and stick model. Black dotted lines for intermolecular hydrogen bonds. (d) Space fill model showing the supramolecular helical structure of tripeptide **2**.

bond (N2–H2···O4) along the crystallographic *b* axis to form an anti-parallel sheet-like structure (Fig. 2b).[39] This anti-parallel sheet-like structure further self-assembled through van der interactions and edge to edge π–π stacking interactions (shortest C–C distance 4.29 Å) along the crystallographic *b* and *c* directions (Fig. 2b).[39] The hydrogen bonding parameters of peptide **1** and **2** are listed in Tables S2 and S3 (ESI†), respectively. The tripeptide **2** forms an intermolecular hydrogen bonded supramolecular helical structure along the crystallographic *c* axis (Fig. 2c).[40] There are three intermolecular hydrogen bonds N2–H2···O4 and O5–H5···O3 (Table S3, ESI†) connecting individual peptide molecules to form the supramolecular helical columns. The C=O and NH groups of Ala and Aib are engaged in intermolecular hydrogen bonding leaving the same hydrogen bonding functionalities of the Tyr residue uninvolved. However, the Tyr side chain OH is in hydrogen bonding with Ala C=O and helps the supramolecular helix formation. The crystal and data collection parameters of peptides **2** are listed in Table S6 (ESI†). Hence, the peptide **1** forms a supramolecular sheet-like structure and peptide **2** forms a supramolecular helix-like structure in higher order assembly.[41]

Moreover, tripeptide **1** forms a transparent gel in toluene, xylene, chlorobenzene and 1,2-dichlorobenzene (Fig. S3, ESI†). The stuff was preliminarily categorized as a gel as it did not obey gravitational flow upon turning the tube upside-down at room temperature. The minimum gelation concentration (MGC) is 5 mg mL^{-1} in 1,2-dichlorobenzene. But, gelation does not occur for tripeptide **2** under the same conditions even at high concentration.

The rheological experiments confirmed the formation of an organogel by tripeptide **1**. From angular frequency measurement at fixed shear strain 0.1%, the storage modulus (G') was found to be larger than the loss modulus (G'') at room temperature (Fig. 3a). This indicates that an entangled fiber network is formed. From shear strain measurement at 25 °C and constant angular frequency (10 rad s^{-1}) LVER 0.15, G' and G'' cross over at 3.9% (Fig. 3b). This indicates the formation of a physically cross-linked organogel through non-covalent interactions.

Initially, the morphology of the tri-peptide organogel was studied by polar optical microscope (POM). A thin slice of the peptide **1** gel was placed on a microscopic glass slide and it was allowed to dry under reduced pressure at room temperature for
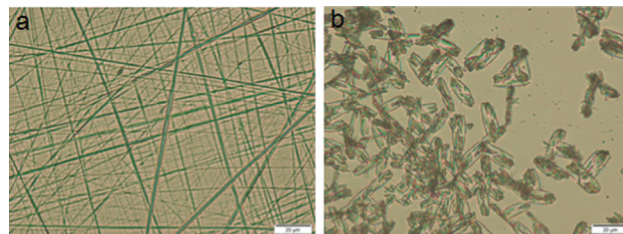
Fig. 4 (a) POM image of peptide **1**. (b) POM image of peptide **2**.

24 h. The POM image shows that peptide 1 forms a wire-like morphology (Fig. 4a). The POM image shows that peptide **2** forms a flake-like morphology (Fig. 4b).

Furthermore, field-emission scanning electron microscopy (FE-SEM) has performed to study the morphology of the tripeptide **1** xerogel. Fig. 5a shows that the peptide forms an entangled fibre-like morphology in gel. The fibers are polydisperse in nature. Fig. 5b shows that the average diameter of peptide 1 fibers is 200 nm and several micrometers long.

The organogel formed by tripeptide **1** in 1,2-dichlorobenzene is so stable that the gel could be suspended by holding one edge and can be shaped into any self-supporting geometrical form.[42] Also, a big organogel block of tripeptide **1** can be chopped into multiple pieces.[43] The organogel formed by tripeptide **1** showed significant self-healing nature. Self-healing is a process of spontaneous formation of a new self-assembling structure when old structures are deceased within a gel. The optical microscopic image exhibits a gradual microscopic healing of a cut gel surface, although the damaged area was still visible (Fig. S4, ESI†). This self-healing experiment exhibits that the organogel is living and dynamic in nature. The FT-IR spectra (Fig. S5, ESI†) of the peptide **1** xerogel exhibit N–H stretching frequency at 3294 cm^{-1} responsible for hydrogen bonded N–H stretching. The band at 3412 cm^{-1} appeared for non hydrogen-bonded N–H. For tripeptide **1**, the ester and amide peaks appeared at 1694 and 1654 cm^{-1}. To identify the driving force of peptide **1** self-assembly, concentration dependent NMR studies were performed on peptide **1** dissolved in deuterated benzene. The concentration dependent ^{1}H NMR study in C$_6$D$_6$ exhibits downfield shift of the Ala NH and Aib NH protons with increasing concentration (Fig. S6, ESI†), which suggests that the NH protons are intermolecularly hydrogen bonded. There is no shift for Phe NH, which suggest that the Phe NH proton is intramolecularly hydrogen bonded. This is consistent with the solid state structure. Moreover, we have
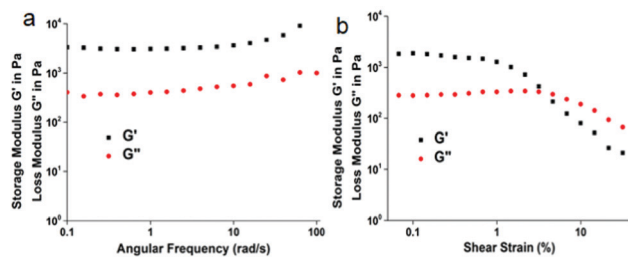

Fig. 3 (a) Storage modulus and loss modulus *vs.* angular frequency for peptide 1 gel in 1,2-dichlorobenzene at 25 °C. (b) Effect of angular strain on the organogel of peptide **1** in 1,2-dichlorobenzene at 25 °C.
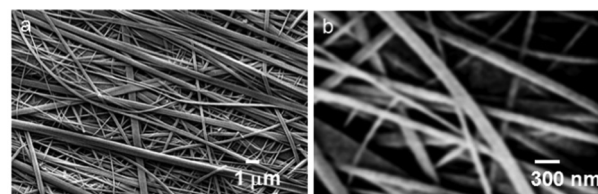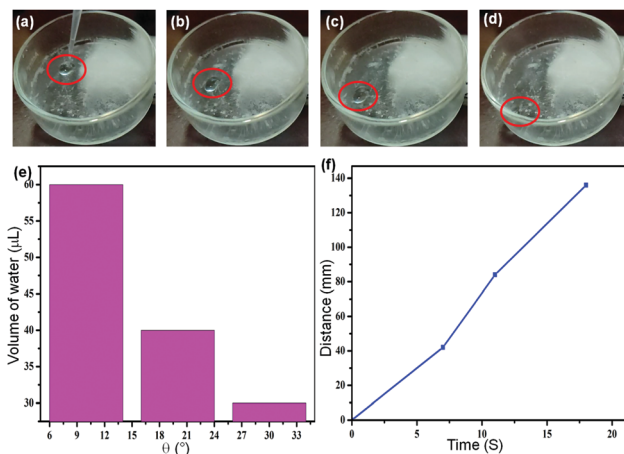

Fig. 5 (a) and (b) FE-SEM image showing entangled fibers of peptide **1** in xerogel.

Fig. 6 (a–d) The movement of the water droplet on the tripeptide **1** organogel surface on 20° tilting. (e) The plot shows the relationship between the volume of the water droplet and the tilting angle of the tripeptide **1** organogel. (f) The plot shows the distance moved by the water droplet concerning the time at 20° tilting angle of tripeptide **1** organogel.

performed CD spectroscopy. The CD spectrum of peptide 1 (Fig. S7, ESI†) has a positive band at 228 nm and negative bands at 216 and 255 nm.

Moreover, the inherent surface properties of the bioinspired tripeptide **1** gel were examined by water adhesion experiment.[6] As shown in Fig. 6a–d, the water droplet (10 μL) slid off the organogel surface at the tilt angle of 20°. The organogel consists of mobile and non-crosslinked components (aromatic solvents in the gel matrices) entrapped within a three-dimensional physically crosslinked gelator network (solid phase). The mobile and solid phases are miscible and the free energy of mixing ($\Delta G = \Delta H - T\Delta S$) is negative ($\Delta G < 0$ for homogenious gel).[15] But, cross-linking of the gel fibers on gelation enhances ΔG, which may trigger demixing (ΔG becomes > 0). Hence the gel surface is dynamic in nature. It has been observed that the velocity of water droplets on inclined organogel surfaces markedly increased with the increasing size of the impregnated water droplet as well as the tilting angle (Fig. 6b). Fig. 6c shows the plot of distance covered by the water droplet with respect to time.

The tripeptide based gel shows an anti-fouling effect against bacteria. The tripeptide 1 and 1,2-dichlorobenzene gel coated paper shows resistance toward bacterial growth (Fig. 7). Fig. 7b shows the growth of *Escherichia coli* colonies on the paper surface coated with only 1,2-dichlorobenzene under aqueous media. Under the same conditions, the tripeptide **1** and 1,2-dichlorobenzene gel coated paper inhibits the growth of *Escherichia coli* on the paper surface (Fig. 7c).

Experimental

Materials

L-Amino acids (L-alanine, L-tyrosine, L-phenylalanine) and α-aminoisobutyric acid were supplied by Sigma chemicals. We have purchased HOBt (1-hydroxybenzotriazole) and DCC
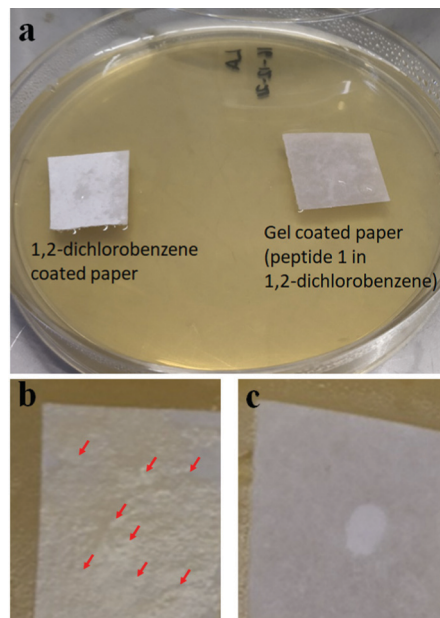
Fig. 7 (a) The anti-fouling experiments (before growth) against *Escherichia coli*. (b) The growth of the *Escherichia coli* colonies (the shiny white spots) on the paper surface coated with only 1,2-dichlorobenzene. (c) Tripeptide 1 gel in 1,2-dichlorobenzene coated paper inhibits the growth of *Escherichia coli*.

(*N*,*N*′-dicyclohexylcarbodiimide) from Sisco Research Laboratories (SRL). The solvents were supplied by Merck.

Peptide synthesis

See ESI.†

NMR experiments

NMR spectra of all the intermediate and final compounds were recorded with a JEOL 400 MHz or Bruker 500 MHz NMR spectrometer. We used CDCl$_3$ or DMSO-d$_6$ as the solvent and TMS as an internal standard.

FT-IR spectroscopy. Solid-state FT-IR spectra were measured with a PerkinElmer Spectrum RX1 spectrophotometer by following the KBr disk technique.

Mass spectrometry. Mass spectra of the final compounds were measured on a Waters Corporation Q–T of Micro YA263 high resolution mass spectrometer by electrospray ionization (positive mode).

Single-crystal X-ray diffraction study. Single-crystal X-ray analysis of the compound was recorded on a Bruker high-resolution X-ray diffractometer with MoKα radiation. Data were processed using the Bruker SAINT package, and the structure solution and refinement procedures were performed using SHELX97. The data have been deposited to CCDC with reference 2106154 and 2106153, respectively.

Gelation. The tripeptide 1 (5 mg) was mixed in 1 mL organic solvent (toluene, xylene, chlorobenzene and 1,2-dichlorobenzene) and a gel was obtained by a heating followed by sonication technique.

Rheology. 5 mg peptide 1 was dissolved in 1 mL 1,2-dichlorobenzene using a 5 mL glass vial for rheology measurement. A gel was obtained by heating followed by sonication for 30 s. The gel was kept at that state for 4 hours before rheology measurement. All rheological measurements were undertaken on an Anton Paar Physica MCR 102 rheometer at 25 °C. Strain and frequency sweeps were performed using a parallel plate geometry. Strain sweeps were performed at 10 rad s^{-1} from 0.01% to 100% strain. Frequency sweeps were carried out from 0.1 rad s^{-1} to 100 rad s^{-1} at 0.1% strain.

Polarized optical microscopy. The morphology of the peptides was determined by using polarized optical microscopy. A small sample of the solution of the compound was placed on a clean glass coverslip and then dried by slow evaporation at room temperature for two days and then visualized at 40× magnification (Olympus optical microscope equipped with a polarizer and a CCD camera).

Field emission scanning electron microscopy. The morphologies of the reported compounds were investigated using field emission-scanning electron microscopy (FE-SEM). For FE-SEM, a small amount of peptide solution or gel was drop cast on a clean glass coverslip and was allowed to dry overnight by slow evaporation at room temperature. Finally, the sample was dried under reduced pressure for two days. The samples were gold-coated, and the micrographs were obtained using a Zeiss DSM 950 scanning electron microscope.

Anti-fouling study. For preparation of media, yeast peptone dextrose (YPD) was placed in a 250 ml flask with 200 ml of media per flask, and then sterilized with an autoclave. After sterilization, it was left to cool, before solidification of the medium, and the content was poured into plates with an average of 20 ml media per plate. The clinical isolates of *Escherichia coli* (TOP10 strain) were grown overnight using a shaking incubator in sterilized YPD media in a test tube before testing and absorbance was measured at 600 nm. The gel of peptide 1 in 1,2-dichlorobenzene was prepared accordingly with a gel concentration of 5 mg ml^{-1} and coated on sterilized white paper (approx. 2 × 2 cm). A paper coated with 1,2-dichlorobenzene was used as a negative control. 100 μL of the prepared culture was spread on the YPD plate, and was incubated at 37 °C for 24 h.

Conclusions

In conclusion, irrespective of the presence of the same peptide backbone, only the side chain hydroxyl functional group has introduced a huge change in the self-assembly and function of analogue peptides. From X-ray crystallography, tripeptide 1 with phenylalanine adopts a β-turn conformation and self-assembles through intermolecular hydrogen bonds to form a supramolecular hydrophobic sheet-like structure. Peptide 1 also forms slippery nanofibers and a gel in aromatic solvents. The resulting gel surfaces show anti-sticking effects against water and exhibit anti-fouling properties. The gel surface inhibits the growth of *Escherichia coli* colonies. Whereas the tyrosine analogue adopts kink like conformations and self-assembles to form a supramolecular helix-like architecture and failed to form a gel. This information may be helpful for fabricating new bioinspired supramolecular functional materials.

Author contributions

K. C. H., S. K. and D. H. planned the experiments. K. C. H. and S. K. carried out the synthesis and experiments. S. M., S. S., A. S. and S. K. N. helped to analyse the data. K. C. H., S. K. and D. H. wrote the paper and S. M., S. S., A. S. and S. K. N. reviewed the paper. All the authors have read and agreed to the published version of the manuscript.

Conflicts of interest

There are no conflicts to declare.

Acknowledgements

Notes and references

1 T. Darmanin and F. Guittard, *Mater. Today*, 2015, **18**, 273.

2 J. G. Tidball, in *Biology of the Integument*, ed. J. Bereiter-Hahn, A. G. Matoltsy and K. S. Richards, Springer, Berlin, 1984, pp. 69–78.

3 C. Neinhuis, K. Koch and W. Barthlott, *Planta*, 2001, **213**, 427.

4 M. Liu, S. Wang and L. Jiang, *Nat. Rev. Mater.*, 2017, **2**, 17036.

5 (*a*) P. Zhang, C. Zhao, T. Zhao, M. Liu and L. Jiang, *Adv. Sci.*, 2019, **6**, 1900996; (*b*) R. Dou, J. Chen, Y. Zhang, X. Wang, D. Cui, Y. Song, L. Jiang and J. Wang, *ACS Appl. Mater. Interfaces*, 2014, **6**, 6998.

6 H. Agarwal, T. J. Polaske, G. Sánchez-Velázquez, H. E. Blackwell and D. M. Lynn, *Chem. Commun.*, 2021, **57**, 12691.

7 S. Hecht and I. Huc, *Foldamers: Structure, Properties, and Applications*, Wiley-VCH, Weinheim, 2007.

8 (*a*) D. Haldar and C. Schmuck, *Chem. Soc. Rev.*, 2009, **2**, 363; (*b*) M. Albrecht, *Chem. Rev.*, 2001, **101**, 3457; (*c*) J. Li, J. A. Wisner and M. C. Jennings, *Org. Lett.*, 2007, **9**, 3267; (*d*) H. Ito, Y. Furusho, T. Hasegawa and E. Yashima, *J. Am. Chem. Soc.*, 2008, **130**, 14008; (*e*) D. Haldar, H. Jiang, J. M. Léger and I. Huc, *Angew. Chem., Int. Ed.*, 2006, **45**, 5483; (*f*) B. Baptiste, J. Zhu, D. Haldar, B. Kauffmann, J. M. Léger and I. Huc, *Chem. – Asian J.*, 2010, **5**, 1364.

9 (a) T. Tu, W. Fang, X. Bao, X. Li and K. H. Dotz, *Angew. Chem., Int. Ed.*, 2011, **50**, 6601; (b) N. Fujita, Y. Sakamoto, M. Shirakawa, M. Ojima, A. Fujii, M. Ozaki and S. Shinkai, *J. Am. Chem. Soc.*, 2007, **129**, 4134.

10 (a) J. J. D. Jong, L. N. Lucas, R. M. Kellogg and J. H. V. Esch, *Science*, 2004, **304**, 278; (b) W. Cai, G. T. Wang, Y. X. Xu, K. Jiang and Z. T. Li, *J. Am. Chem. Soc.*, 2008, **130**, 6936.

11 O. J. Dautel, M. Robitzer, J. P. L. Porte, F. S. Spirau and J. J. E. Moreau, *J. Am. Chem. Soc.*, 2006, **128**, 16213.

12 G. Cravotto and P. Cintas, *Chem. Soc. Rev.*, 2009, **38**, 2684.

13 C. Dou, D. Li, H. Gao, C. Wang, H. Zhang and Y. Wang, *Langmuir*, 2010, **26**, 2113.

14 K. Isozaki, H. Takaya and T. Naota, *Angew. Chem., Int. Ed.*, 2007, **46**, 2855.

15 A. Ajayaghosh, P. Chithra and R. Varghese, *Angew. Chem., Int. Ed.*, 2007, **46**, 230.

16 H. J. Kim, J. H. Lee and M. Lee, *Angew. Chem., Int. Ed.*, 2005, **44**, 5810.

17 S. Basak, J. Nanda and A. Banerjee, *J. Mater. Chem.*, 2012, **22**, 11658.

18 D. M. Wood, B. W. Greenland, A. L. Acton, F. Rodr′ıguez-Llansola, C. A. Murray, C. J. Cardin, J. F. Miravet, B. Escuder, I. W. Hamley and W. Hayes, *Chem. – Eur. J.*, 2012, **18**, 2692.

19 S. Basak, N. Nandi, S. Paul, I. W. Hamley and A. Banerjee, *Chem. Commun.*, 2017, **53**, 5910.

20 B. O. Okesola and D. K. Smith, *Chem. Commun.*, 2013, **49**, 11164.

21 P. Chakraborty, B. Roy, P. Bairi and A. K. Nandi, *J. Mater. Chem.*, 2012, **22**, 20291.

22 S. Sengupta and R. Mondal, *J. Mater. Chem. A*, 2014, **2**, 16373.

23 A. Chakrabarty, U. Maitra and A. D. Das, *J. Mater. Chem.*, 2012, **22**, 18268.

24 N. Cheng, Q. Hu, Y. Guo, Y. Wang and L. Yu, *ACS Appl. Mater. Interfaces*, 2015, **7**, 10258.

25 M. Tena-Solsona, J. Nanda, S. D′ıaz-Oltra, A. Chotera, G. Ashkenasy and B. Escuder, *Chem. – Eur. J.*, 2016, **22**, 6687.

26 B. Escuder, F. Rodríguez-Llansola and J. F. Miravet, *New J. Chem.*, 2010, **34**, 1044.

27 W. Kubo, T. Kitamura, K. Hanabusa, Y. Wada and S. Yanagida, *Chem. Commun.*, 2002, 374.

28 J. H. Jung, H. Kobayashi, M. Masuda, T. Shimizu and S. Shinkai, *J. Am. Chem. Soc.*, 2001, **123**, 8785.

29 E. D. Sone, E. R. Zubarev and S. I. Stupp, *Angew. Chem., Int. Ed.*, 2002, **41**, 1705.

30 S. Kobayashi, N. Hamasaki, M. Suzuki, M. Kimura, H. Shinkai and K. Hanabusa, *J. Am. Chem. Soc.*, 2002, **124**, 6550.

31 P. Xue, R. Lu, Y. Huang, M. Jin, C. Tan, C. Bao, Z. Wang and Y. Zhao, *Langmuir*, 2004, **20**, 6470.

32 S. Kobayashi, K. Hanabusa, N. Hamasaki, M. Kimura, H. Shirai and S. Shinkai, *Chem. Mater.*, 2000, **12**, 1523.

33 Y. Yamada and J. P. Schneider, *Biomacromolecules*, 2016, **17**, 2634.

34 S. R. Jadhav, B. S. Chiou, D. F. Wood, G. DeGrande Hoffman, G. M. Glenn and G. John, *Soft Matter*, 2011, 7, 864.

35 K. Basu, A. Baral, S. Basak, A. Dehsorkhi, J. Nanda, D. Bhunia, S. Ghosh, V. Castelletto, I. W. Hamley and A. Banerjee, *Chem. Commun.*, 2016, **52**, 5045.

36 C. H. Gorbitz, *Chem. – Eur. J.*, 2007, **13**, 1022.

37 (a) Y. Liu, Y. Wang, L. Jin, T. Chen and B. Yin, *Soft Matter*, 2016, **12**, 934; (b) E. Azuma, K. Kuramochi and K. Tsubaki, *Chem. Pharm. Bull.*, 2010, **58**, 680; (c) D. Podder, S. Roy Chowdhury, S. K. Nandi and D. Haldar, *New J. Chem.*, 2019, **43**, 3743; (d) S. Basak, N. Nandi, S. Paul, I. W. Hamley and A. Banerjee, *Chem. Commun.*, 2017, **53**, 5910.

38 A. K. Das, A. Banerjee, M. G. B. Drew, S. Ray, D. Haldar and A. Banerjee, *Tetrahedron*, 2005, **61**, 5027.

39 A. Banerjee, S. K. Maji, M. G. B. Drew, D. Haldar and A. Banerjee, *Tetrahedron Lett.*, 2003, **44**, 6741.

40 D. Haldar, S. K. Maji, M. G. B. Drew, A. Banerjee and A. Banerjee, *Tetrahedron Lett.*, 2002, **43**, 5465–5468.

41 M. A. Spackman and J. J. McKinnon, *CrystEngComm*, 2002, **4**, 378.

42 A. Vidyasagar, K. Handore and K. M. Sureshan, *Angew. Chem., Int. Ed.*, 2011, **50**, 8021.

43 T. Das, M. Haring, D. Haldar and D. D. Diaz, *Biomater. Sci.*, 2018, **6**, 38.